ISSN 2176-5480

22nd International Congress of Mechanical Engineering (COBEM 2013)
November 3-7, 2013, Ribeirão Preto, SP, Brazil

INFLUENCE OF THE TRANSVERSAL SHEAR EFFECTS ON STRUCTURAL ANALYSIS OF AIRCRAFT TAILS

Murilo Sartorato
Volnei Tita
University of São Paulo, São Carlos School of Engineering, Department of Aeronautical Engineering, Av. João Dagnone, 1100 São Carlos, SP, Brazil
murilosart@gmail.com, voltita@sc.usp.br

Abstract. *The effects of transversal shear stresses on shell structures are partly governed by the thickness of the plate and are usually neglectable. In fact, in the most applications, thin plates are preferred. However, particularly in the aeronautical industry, there are some aircraft structures and dynamic analysis where the transversal shear effects are significant, such empennages due to their increased thickness in the leading edge due to bird-strike requirements – especially in composite fiber-glass-epoxy and/or carbon-epoxy laminates. Thus, the correct approach for the transversal shear effects is necessary for thick composite laminate structures. The introduction of shear correction factors can circumvent this problem by mathematically simulating the transversal shear distribution over the thickness of laminates. Nonetheless, these factors are difficult to obtain analytically or experimentally in composite materials due to the large number of variables in composite structures compared to isotropic materials; e.g. layup properties, fiber arrangements, orientation of the layers and others. This paper presents a methodology to calculate the shear correction factors for composite laminates using a Representative Element Volume (REV) approach, which is solved by finite element analyses. The results are obtained for two examples: a carbon-epoxy laminate made of UD layers and a glass-epoxy laminate made of BD layers (plain woven). Finally, as a case study, a composite vertical tail structure of an aircraft was modeled using ABAQUS finite element package, considering impact tests. The analyses were made using the default theories present in the software as well as incorporating the shear correction factors previously calculated. Lastly, a discussion of the results and consequently implications in an aircraft structural design is made.*

Keywords: *Composite materials; representative volume element (RVE); transversal shear effects; finite element analysis; impact analysis*

1. INTRODUCTION

In the aeronautical industries, due to several issues such as: structure requirements, necessity for low weight and easiness of manufacture, most structural elements, even primary ones such as spars, are made from thin plates. The effects of transversal shear stresses on shell structures are partly governed by its thickness and are usually neglectable for thin structures. However, there are particular structural elements or analysis in which the transversal shear effects are significant as in wing stubs, high vibration modes of wings and tails, and impact analysis. Also, as one considers composite materials, the values of both transversal shear stresses and distortions are important, as they govern effects in failure phenomena such as deboning and interface failure (delamination) (Reddy and Ochoa, 1993). Furthermore, there are some structures, which use thick composite plates as a primary structural element, for example stubs, tail support structures and leading edge of vertical tails in airplanes and tail-rotor support structures in helicopters.

In numerical analysis, in particular in Finite Element Analysis (FEA), the correct prediction and numerical simulation of the mechanical behavior of composite laminate plates largely depend on the theory used to model the structure (Reddy and Arciniega, 2004).

For one side, most commercial finite element packages use elements based either on the Classical Laminate Theory or the First Order Shear Theory. The first is based on the Kirchhoff plate kinematic hypothesis, which completely neglects transversal shear effects. The second is usually based upon the Reisner/Mindlin plate kinematic hypothesis, however this theory creates over stiffness for the transversal efforts and use the assumption that the transversal shear stress distribution through the thickness of a plate (isotropic or laminated) is given by a parabola. This last assumption is usually not true for both laminated materials or even for isotropic materials given that the external efforts are not uniform over the thickness of the structure, such as in bending situations (Reddy and Ochoa, 1993).

To account for the correct and non-uniform distribution of the transversal shear stresses, several High-Order Shear Theories were created in the last decades and can be found in the literature. A good review of such methods was made by Qatu et al. (2010). Yet, finite elements formulated using these theories lead to larger computational times, and can be problematic to use in large models or taxing analysis such as impact tests. As such, another solution has been created: the introduction of coefficients defined as shear correction factors or transversal shear stiffnesses in the transversal shear constitutive matrix. These coefficients can mathematically simulate non-parabolic distributions of transversal stresses. However, for composite materials, these are difficult to be calculated due to being highly dependent on several

ISSN 2176-5480

properties such as: structure geometry; external load over the structure; laminate lay-up properties and geometry of the fibers.

Also, several commercial finite element packages, such as Abaqus, Ansys and Nastran provide the option to manually input the shear correction factors, even for laminated composite materials. As such, even though more powerful models have been developed, the correct stimulation of these coefficients is still an important and open problem.

This paper presents a methodology to calculate the shear correction factors for unidirectional (UD layers) and plain woven bidirectional (BD layers) composites with 0°, 45° or 90° orientated layers. This is done by calculating the shear correction factors solving a Representative Volume Element (RVE) problem for a given laminate through a Finite Element Analyses (FEA) approach. The methodology is then applied to two different examples: a carbon-epoxy composite laminate made of unidirectional (UD) layers and a glass-epoxy laminate made of bidirectional (BD) plain woven layers. Results for the analyses of the RVE of both examples are presented. The calculated shear correction factors are compared to analytical models found in the literature. Finally, as a case study, a composite vertical tail structure of an aircraft was modeled using ABAQUS finite element package, considering modal analysis and impact tests. The analyses were made using the default theories presented in the software as well as incorporating the shear correction factors previously calculated. Lastly, a discussion of the results and consequently implications in an aircraft structural design is made.

2. PROPOSED METHODOLOGY

In this section, the proposed methodology for the calculation of the shear corretion factors is briefly explained Innitially, the basic assumptions used are summarized. Then the hypothesis needed for the creation of the RVE, such as the periodic boundary conditions, are made. The implications of the layers orientations on the methodology are discussed.

2.1 Constitutive Equations

Assuming that transversal shear effects are compactible with the laminate mechanical behavior, and its displacements description is given by either the First Order Shear Theory or any Higher-Order Shear Theory, the classic ABBD composite constitutive matrix obtained from the Classical Theory of Laminates can be expanded to integrate the effects of transversal shear distortions (γ). According to Reddy and Ochoa (1993), for the first order shear theory, this extended matrix can be written as Eq. (1), where: F is the membrane generalized efforts over the laminate; M are the generalized bending efforts; Q are the generalized shear efforts, A, B, D and G are the different order matrixes that together constitue the laminate constitutive matrix; ε are the middle surface planal strains, γ are the middle surface distortions and κ are the middle surface curvatures.

$$\begin{Bmatrix} F \\ M \\ Q \end{Bmatrix} = \begin{bmatrix} A & B & 0 \\ B & D & 0 \\ 0 & 0 & G \end{bmatrix} \begin{Bmatrix} \varepsilon \\ \kappa \\ \gamma \end{Bmatrix} \tag{1}$$

Pai (1995) described the transversal shear distribution over the thickness of the laminate using fifth-order polinomials functions. This way, the researcher proved that the transversal effects terms found in both first and higher-order shear theories may be written as Eq. (2) by introducing the k_1, k_2 and k_3 shear correction factors into the G matrix.

$$\begin{Bmatrix} \overline{Q}_x \\ \overline{Q}_y \end{Bmatrix} = \begin{bmatrix} k_1 \hat{A}_{44} & k_3 \hat{A}_{45} \\ k_3 \hat{A}_{54} & k_2 \hat{A}_{55} \end{bmatrix} \begin{Bmatrix} \gamma_{xz} \\ \gamma_{yz} \end{Bmatrix} \tag{2}$$

where k_1, k_2 and k_3 are the shear correction factors; $\bar{Q}_x$, $\bar{Q}_y$, are the resultant shearing loads over the boundaries; $\hat{A}_{44}$, $\hat{A}_{45}$ and $\hat{A}_{55}$ are the coefficients of the G matrix; and $\bar{\gamma}_{xz}$, $\bar{\gamma}_{yz}$ are the distortions of the laminate plate averaged by the specific strain energy over the whole thickness for a specific laminate.

The proposed methodology is based on the assumption that Eq. (2) is valid for a finite element model of a heterogeneous microstructure of a given composite laminate, as long as the quantities used are averaged over the strain energy quantities for each element. Using this assumption, in particular for the cases of UD and BD composites, it is possible to create a solid finite element model of a cuboid RVE that models the whole thickness of the laminate. It should be noted that, due geometric limitations of the repeating structure lengths, only RVEs containing layers with 0°, 45° or 90° orientations may be modeled in a RVE such as a cuboid is created. As such, by doing a FEA of this RVE the energy averaged quantities $\bar{\gamma}_{xy}$, $\bar{\gamma}_{zy}$ may be calculated using Eqs. (3) and (4).

ISSN 2176-5480

$$\bar{\gamma}_{xz} = \frac{\sum_{i=1}^{n}\sum_{j=1}^{g}\sum_{k=1}^{6}\gamma_{xz_{ij}}\varepsilon_{k_{ij}}\sigma_{k_{ij}}}{\sum_{i=1}^{n}\sum_{j=1}^{g}\sum_{k=1}^{6}\varepsilon_{k_{ij}}\sigma_{k_{ij}}} \tag{3}$$

$$\bar{\gamma}_{yz} = \frac{\sum_{i=1}^{n}\sum_{j=1}^{g}\sum_{k=1}^{6}\gamma_{yz_{ij}}\varepsilon_{k_{ij}}\sigma_{k_{ij}}}{\sum_{i=1}^{n}\sum_{j=1}^{g}\sum_{k=1}^{6}\varepsilon_{k_{ij}}\sigma_{k_{ij}}} \tag{4}$$

where n is the number of the finite elements in the RVE and, g is the number of the integration points per finite element. The homogenized properties of the laminate $\hat{A}_{44}$, $\hat{A}_{45}$ and $\hat{A}_{55}$ can be obtained by the Rule of Mixtures in conjunction to the First-Order Shear Theory applied for laminates. Therefore, the problem of the determination of the shear correction factors is simplified into a linear system.

2.2 Representative volume element and periodic boundary conditions

According to Pindera et al. (2004), the definition of an RVE is smallest size of a properly bounded unit cell contained in the micro structure of a given material that can represent the whole that material behavior. In general, this approach is used to obtain effective or homogenized macroscopic material properties.

In this work, however, the term RVE is being used outside its formal definition, as the chosen unit cell is of the same order of magnitude of the thickness of the laminate plate. In this case, some researchers prefer to use the term Repeating Unit Cell (RUC), but, in general, these terms are used interchangeably. Moreover, the methodology remains valid, because the objective consists on calculating the averaged strain distortions over the volume strain energy, which are global quantities and depend on the stresses and strains distributions through the whole thickness.

For a better definition of the periodic boundary needed for a cuboid RVE of a UD or BD composite, its faces are named as such: the faces in the direction transversal to the fibers are called y^+ and y^- and the faces perpendicular to those are called x^+, x^-, z^+ and z^-. This nomenclature is shown in Fig. 1.

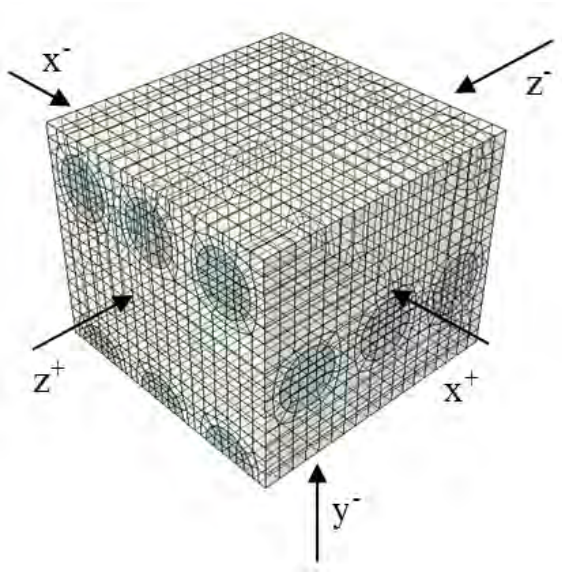

Figure 1. Cuboid RVE faces nomenclature

There are several ways to apply the periodic boundary conditions at a given RVE. The form used in this work is given by Eqs. (5) to (7), which guarantee the periodicity and parallel deformation between the faces, and is specific to cuboids RVEs (Xia et al., 2003): the displacement within a given face is equal to the sum of the displacement for its opposite face summed to mechanical behavior of the volume between both faces.

$$u_i^{x^+} = u_i^{x^-} + \bar{S}_{ij} L_j^x \tag{5}$$

$$u_i^{y^+} = u_i^{y^-} + \bar{S}_{ij} L_j^y \tag{6}$$

ISSN 2176-5480

$$u_i^{z^+} = u_i^{z^-} + \overline{S}_{ij} L_j^z \tag{7}$$

Where $\overline{S}_{ij}$ is the equivalent stress-strain tensor of the RVE and Lj is the distance between the two opposite nodes in the undeformed state. As the $\overline{S}_{ij}$ tensor is hard to be calculated, these equations may be written for every pairs of nodes A, B and C, D in opposite faces as shown by Eq. 8 (Xia et al., 2003).

$$u_i^A - u_i^B = u_i^C - u_i^D \tag{8}$$

3. CASE STUDIES

3.1 RVE Examples

Two examples were investigated in order to evaluate the potentials and limitations of the proposed methodology.

The first consisted on a laminate plate made of UD layers of carbon-epoxy composite with [0°/90°/0°/90°/0°] lay-up. Also, the total thickness is equal 1.75 mm and the matrix volume fraction is about 37.7%. The second consisted on a laminate plate made of BD plain woven layers of glass-epoxy with $[(0°/90°)_3(+45°/-45°)]_S$ lay-up. Also, the total thickness is equal 2.0 mm and the matrix volume fraction is 32.3%.

The material properties for fibers and matrixes used in the simulations can be found in Tab. 1. It is important to mention that the matrix and the fibers were considered linear elastic as well as isotropic materials during the numerical analyses.

Table 1. Properties used for each case study

Property	First Example Composite		Second Example Composite	
	Epoxy Matrix	Carbon Fibre	Epoxy Matrix	Glass Fibre
E [GPa]	3.2	210	4.0	72
ν	0.38	0.11	0.40	0.22
ρ [kg/m^3]	1200	1780	1300	2560

Figure 2 shows the RVE used for both examples evaluated. These RVEs were modeled via Abaqus, using quadratic solid tetrahedron and hexagonal elements (C3D20 and C3D10). The quadratic elements were chosen in order to obtain better prediction of the transversal strain and stresses, which are the primary quantities used in the shear corrections factors calculation and are secondary results of the analysis.

For the plain woven RVE (second example – BD layers), the curvature and geometry of the weave were created using CAD software, based upon the thickness of a single layer and the published works of Barbero et al. (2005) and Potluri and Thammandra (2007). The CAD drawings of the 90° and 45° layers are shown in Fig. 3a and 3b.

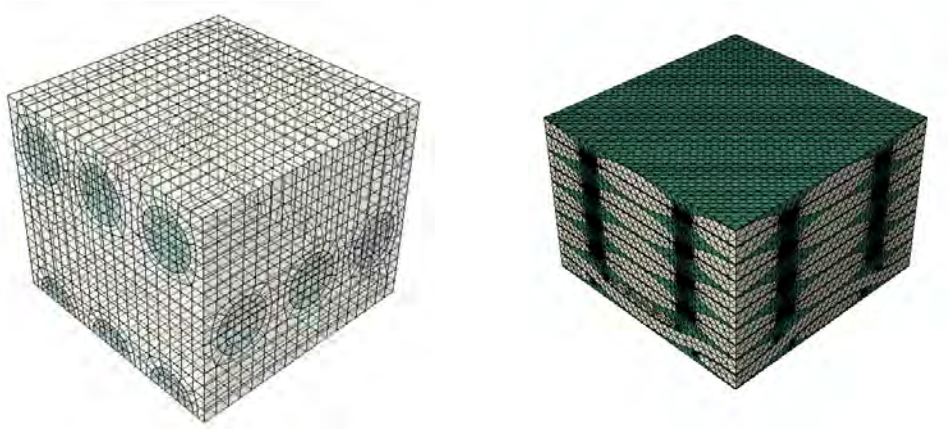

a b

Figure 2. RVEs: a) RVE 1 - First example (UD layers); b) RVE 2- Second example (BD layers)

ISSN 2176-5480

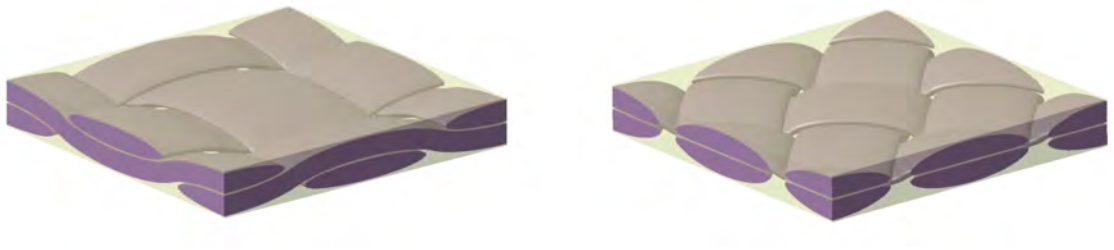

a b

Figure 3. CAD drawing of the 0° (a) and 45° (b) layers used in the RVE 2 of the second case study

In both analyses, the laminate symmetry was used to decrease the number of elements in the model. Therefore, it was developed only a half of the laminate plate and, symmetry conditions were applied ($u_2 = \theta_1 = \theta_3 = 0$). Also, a positive shear traction load in the zy/xy planes was applied in the respective pair of faces. Thus, analogously, a negative shear load was applied to the face y+ to complete the equilibrium of the efforts over the RVE. The full set of boundary conditions is outlined in Fig. 4.

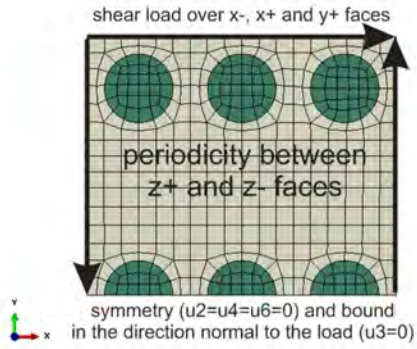

Figure 4. Boundary conditions applied at the RVE 1 for the first finite element analysis.

It should be noted that the correct inversion of BCs application depends if laminate is balanced or unbalanced. For unbalanced composites, such as the one in the first example (UD layers) in addition to the boundary conditions inversion between the x and z pair of faces, it is necessary to change the magnitude of the shear efforts applied.

3.2 Empenagge Case Study

Using the proposed methodology in the calculation of shear correction factors, its influence in real structure design structures was evaluated using a virtual, simplified model of an aircraft vertical tail manufactured with the glass-epoxy composite of the second example above. Modal analysis of the main box structure of the tail and an impact analysis test based upon the FAR 25 bird strike requirements were made using the finite element analysis using both the default shear models present in Abaqus for the S4R shell element and the calculated shear correction factor from the RVE analyses. The S4R element considers the classical parabolic distribution, which for isotropic materials generates the Reissner/Mindlin solution of $k_1 = k_2 = 5/6, k_3 = 0$.

The idealized empenagge, found in Fig. 5, used dimensions and design angles commonly found in the light-jet class of aircrafts, which are prone to the use of glass-fiber in the leading-edges and have operational conditions and structural dimensions that benefit the transversal shear effects such as the high swept angle. The root chord was set to 2.5 m, the tip chord 0.9 m and a 45° swept angle. A NACA 0012 airfoil was used to model the external shape of the tail. The model also has two spars, set on 13% and 70% of the chord, and six evenly distancied ribs.

ISSN 2176-5480

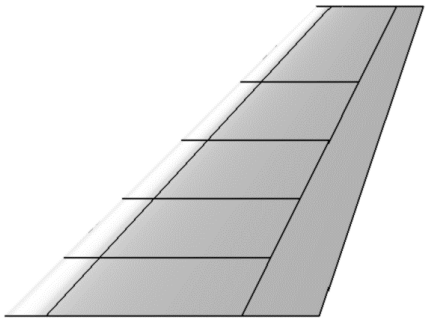

Figure 5. Idealized vertical tail structure used in the case study.

The finite element model used for the modal analysis are found in Fig. 6 and 6b. The boundary conditions applied to the model were the encastre of the root of the spars and pin of the borders of the first rib. This was done to both simulate the presence of the fuselage over the tail as well as to avoid the Saint-Venant effects.

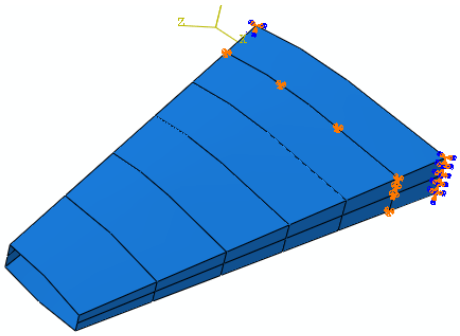

Figure 6. FEA model of the idealized vertical tail main box structure used for the modal analysis.

For the impact analysis, a small part of the empenagge featuring the leading edge; first spar; second, third and fourth ribs; and a slight extended skin area was used. The model and its mesh are shown in Figs. 7a and 7b. As boundary conditions the root of the leading edge and the spar were pinned, while on the surface edges of the skin were applied material continuity conditions. The mass and diameter of the projectile were according to FAR 25 bird strike regulations: mass of 3.62874 kg (8 lb), with a 0.20 m diameter, and its initial velocity was set as 51.5 m/s (100 knots), common approach speed for the said category. The impact region was chosen to be over the third rib, as this is the condition prone to the highest transversal shear effects. The mesh used was sparse in the regions farther from the impact and concentrated in the region of the impact. A 'hard', frictionless contact model was used for the impact. The simulation was run until the projectile completely stopped, which was aproximally 0.01 s.

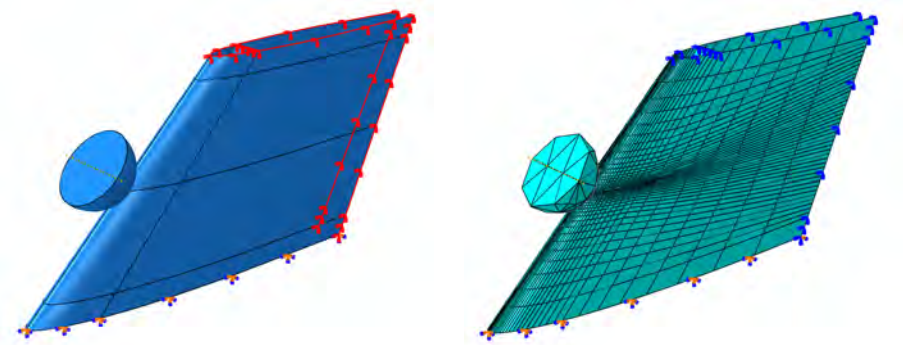

a b

Figure 7. FEA model used for the impact analysis: a) geometric model; b) mesh and boundary conditions.

ISSN 2176-5480

4. RESULTS

4.1 Results of the FEA for each RVE

Figure 7 shows the deformed shape and the distribution of the transversal strains for each FEA. Fig.7a shows the γ_{13} distribution for the first finite element analysis and, Fig. 7b shows the γ_{23} for the second finite element analysis, considering the RVE 1 (UD layers). Similar results for the RVE 2 (BD layers) can be found in the Fig.8. in these images the periodic boundary conditions, that is, the parallel deformation between opposites faces, can be seem. Also, the concentration of the shear distortions in the matrix phase can be observed. This phenomena occurs particularly in the interface between the matrix and the fibres region and is an indication that further works much study the influence of non-perfect contact models for the interface in the present methodology.

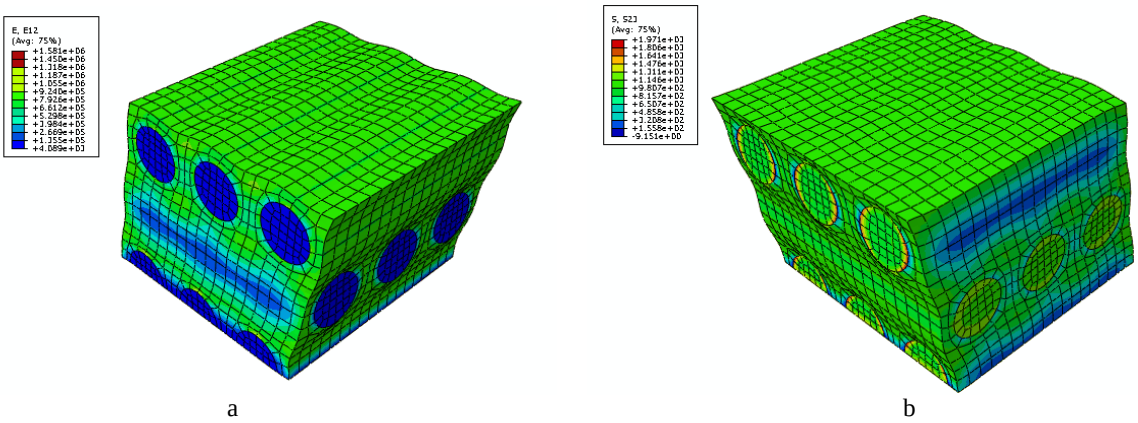

a b

Figure 7. Results for the first example (UD, carbon-epoxy): a) distribution of γ_{13} in the first finite element analysis; b) distribution of γ_{23} in the second finite element analysis.

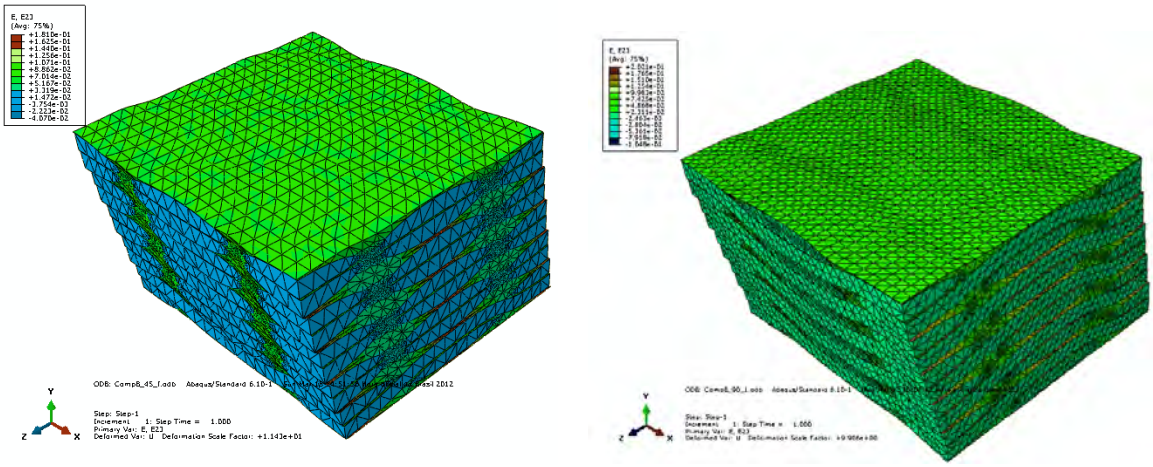

a b

Figure 8. Results for the second example (BD, woven glass-epoxy): a) distribution of γ_{13} in the first finite element analysis; b) distribution of γ_{23} in the second finite element analysis

Based on the distribution of strains in the Fig. 9, it is possible to observe that the common estimation based on a parabola is not realistic, because the real distribution has a complex shape. Moreover, from this distribution, it can be seen that the regions with resin and fibre are easily discerned, as the greater deformations occur in the small portions of resin, which have lower stiffness.

ISSN 2176-5480

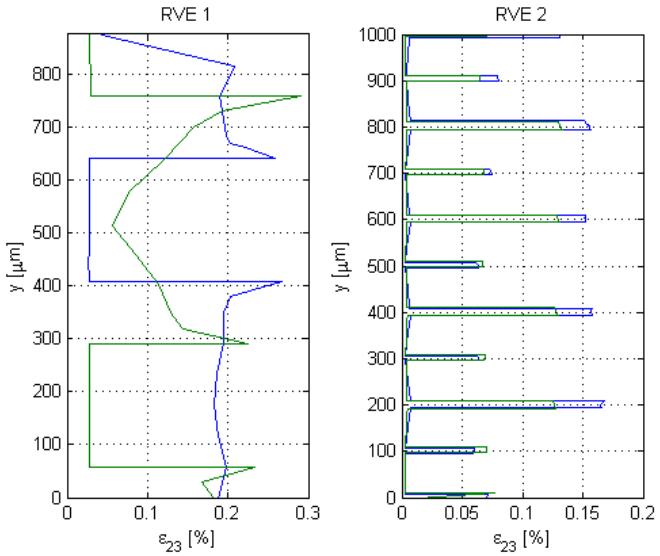

Figure 9. γ_{23} distribution for both case studies: RVE 1 and RVE 2

4.2 Shear correction factors calculation

Based on the FEA results, it is possible to calculate the shear correction factors using the Eq. 2. Thus, Tab. 2 shows the results calculated for the shear correction factors, using the methodology proposal for the UD example. Table 3 shows the results for the BD example. Few works in the literature can be used to compare the obtained results due to the existing models not being completely general. Most of them are semi-empirical, or adjusted for the specific lay-ups being studied by the researchers. Two models found on the literature that provided a general solution for the problem were used to compare the results with the present work and are found in Tab. 2 and 3.

Table 2. Results of the shear correction factors for the first case study (UD layers): methodology proposal vs. Literature

Model	K1	K2	K3
Present work	0.7369	0.7369	-
Pai (1995)	0.7031	0.8676	0.7810
Raman and Davalos (1996)	0.7909	0.7909	-

Table 3. Results of the shear correction factors for the second case study (BD layers): methodology proposal vs. Literature

Model	K1	K2	K3
Present work	0.8413	0.8413	2.143
Pai (1995)	0.8676	0.8676	1.731
Sartorato e Tita (2011)	0.8343	0.8343	-

For the first case study (UD layers), due to it only having layers with 0° or 90° orientation, $\hat{A}_{45} = 0$. Hence, in this case, by the current model, $k_1=k_2$ and k_3 cannot be defined. For the second case study (BD layers), as the composite contains layers not aligned with the axis (45° and -45°), $\hat{A}_{45} \neq 0$, however, as the laminate is balanced, i.e. there is at least two symmetry planes perpendicular to the xz plane, $k_1=k_2$ as shown by Table 3.

The results obtained are difficult to analyze, as there is no analytical solution for the problem. Also, there are discrepant results provided by the models found in the literature. For the second example the results obtained were close to the classical Reissner/Mindlin solution of $k_1=k_2=0.8333$, however the values of k_3 are large. This is expected as the due to the woven of the fibers, a large coupling between the distortion effects in the two different planes (xy and yz) should exist. For the first case study, the obtained coefficients were smaller than the classical solutions. This fact can be explained due to the composite being unbalanced.

ISSN 2176-5480

4.3 Modal Analysis of the Case Study

Table 4 shows the calculated natural frequencies for the FEA model of the vertical tail analyzed. The percentage difference between the analysis using Abaqus' default model for the transversal shear and using the shear correction factors obtained using the present work methodology are show. A small percentual difference between the models was observed, as the calculated frequencies were between maximum percentual differences of 3%. As the shear correction factors found for the structure material were larger than the classical Reissner/Mindlin solution, it was predictable that the results for the model using these obtained coefficients would have smaller natural frequencies. This can be explained as greater shear correction factors can be interpreted as a stiffening effect in the structure in comparison to the classic model.

Also, it should be noted that for the higher modes of vibration, the absolute difference between the frequencies was changed for up to 30 Hz. This change can have great importance for some applications such as structure health monitoring and aeroelastic effects prediction.

Table 4. Numerical results for the natural frequencies of the idealized tail structure using Abaqus' default model and the results for shear correction factors using the present work methodology

Mode		1.0	2.0	3.0	4.0	5.0	6.0	7.0	8.0
Frequency	Abaqus Default	106.2	180.0	201.3	364.3	401.9	450.8	529.7	585.9
	Present Work	104.8	177.1	200.5	357.8	395.2	440.9	528.1	575.4
% Difference*		1.347%	1.670%	0.354%	1.808%	1.713%	2.249%	0.309%	1.817%
Mode		9.0	10.0	11.0	12.0	13.0	14.0	15.0	16.0
Frequency	Abaqus Default	667.9	682.3	711.1	726.4	838.1	917.2	971.9	1016
	Present Work	655.5	676.6	705.2	713.8	826.2	895.9	953.2	986.4
% Difference*		1.882%	0.834%	0.834%	1.764%	1.448%	2.376%	1.955%	2.999%

$$* \left| \frac{\omega_{Abaqus} - \omega_{PresentWork}}{\omega_{PresentWork}} \right| * 100$$

4.4 Impact Analysis of the Case Study

Figure 10 shows the history of the displacement of the impact point in the FEA model for the analysis using both Abaqus' default transversal shear model and the present work solution for the shear correction factors. The strange behavior of the displacement of the impact point in both analyses can be explained by the impact occurring over a rib. Due to this area greater stiffness, the projectile was dislocated to the region between two ribs due the impact. As such, during the "slip" of the projectile, the impact point displacement suffered a decrease, after that, as the whole structure was being deformed, the displacement started to increase for a second time.

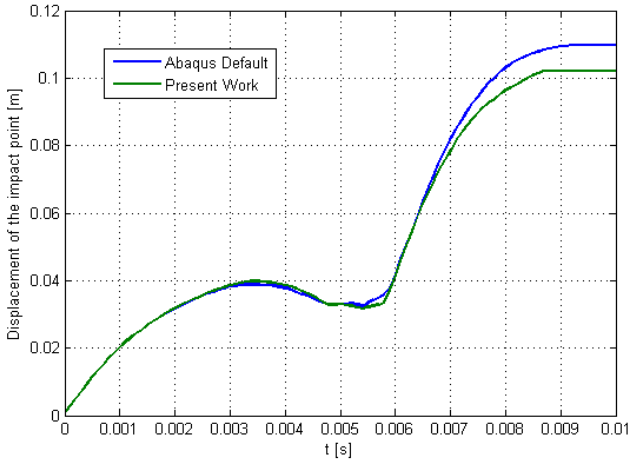

Figure 10. Displacement evolution of the impact point.

ISSN 2176-5480

It can be observed that during most of the impact duration, the difference in the displacements is neglectable. The two time regions where the models start to differ are during the projectile "slip" and the final movements of the structure. The final displacement of the structure had a great difference of 7.01%, between 0.1021 m and 0.1098 m.

Figure 11 shows the evolution of the strain energy in the whole tail for the duration of the impact. Both the total impact energy and the final absorbed energy in the structure were different by the use of the present methodology shear correction factors.

Figure 12 shows a close of the total impact energy peak. It should be noted that for both cases, the strain energy absorbed by the structure is larger than the total impact energy of the projectile, equal to 4719.1 J. This fact can be explained due to the model not having coupled thermal and acoustic formulations, not having a material damage model, and the frictionless contact model used. By not using these more complex models, most of the energy dissipation sources are absent, numerically generating artificial strain energy. In the case of the full impact energy, the use of the calculated shear correction factors showed a 4.028% greater maximum impact energy, which should be attributed by the increase in the stiffness of the model, due to larger than the classical theory coefficients.

As for the absorbed impact, the present work model calculated a 10.04% smaller energy in the structure. This can be explained by the presence of the k_3 coefficient, which does not exist in the classical theory. The coupling caused by this coefficient between both transversal shear efforts makes a larger energy dissipation occur in the analysis using the present work solution

These differences in the calculated impact energies can lead to huge effects in the design of such structures as, if the impact requeriments are the limitating aspects of the design, most design metrics use the absorved impact energy for the calculation of safety coeficients.

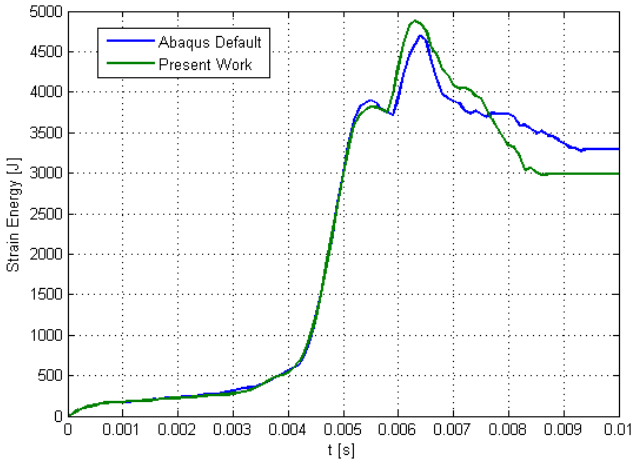

Figure 11. Total strain energy evolution during impact.

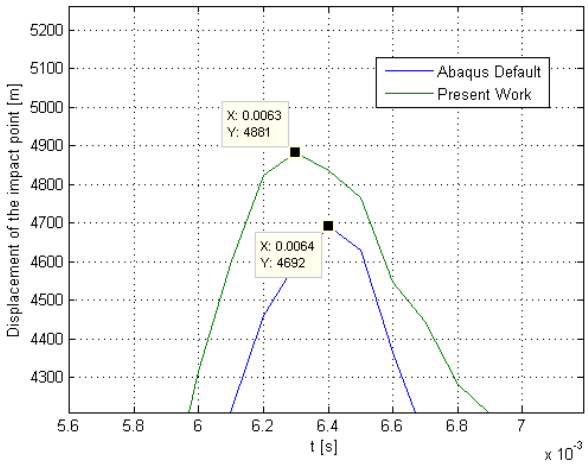

Figure 12. Close of the maximum impact energy.

ISSN 2176-5480

5. CONCLUSIONS

In the present work a methodology for the calculation of shear correction factors for laminate plates with UD and BD layers with 0°, 45° or 90° oriented layers was presented using a RVE approach. Also, the constitutive equations of the methodology were discussed. The periodic boundary conditions and the suitable application of the boundary conditions and loads for the RVE were presented and discussed in details.

Two example composite laminates, one with carbon-epoxy UD layers and a second with woven glass-epoxy layers were made using the proposed methodology. Results for shear correction factors were compared to results obtained by models provided at the literature. While the results were distant from each other, a deeper analysis is difficult to be performed as few models for the calculation of such coefficients exist within the literature.

Finally, a study showing the influence of different shear correction factors in practical strucures was carried out by the modal analyses and impact test of a idealized aircraft vertical tail strucuture manufactured with the same material used in the second example.

For the results of the modal analysis, the influence of the shear correction factors was small, changing the found natural frequencies of the structures at most by 3%. Yet, these results can have significancy in some studies, such as passive vibration control, structure health monitorin and aeroelastic effects predition, as these small changes can influence the control meshs, circuits and sensor/actuators in the design of such philosofies.

For the impact test results, a large difference in the total impact energy and absorved energy of the structure was observed. This can lead to huge effects in the design of such structures as, if the impact requeriments are the limitating aspects of the design, most design metrics use the absorved impact energy for the calculation of safety coeficients. However, it should be noted that the analysis made in the present work was did not include energy dissipations by heat, accoustic and material damage. As such, future studies using the same proposed problem with more complex and powerful contact and energy methods, and aditional damage models should be made, as well as tests comparing the numerical results to experimental data.

Nonetheless, it can be concluded that the shear correction factors have a significant influence on the response of composite structures. And, the methodology proposal can be an alternative to estimate with more accuracy not only shear correction factors, but also the response of composite structures and can have influences in structural design.

6. ACKNOWLEDGEMENTS

The authors would like to thank Research Foundation of State of Sao Paulo FAPESP (process number: 10/13596-0) as well as to thank Prof. Reginaldo Teixeira Coelho from Engineering School of São Carlos (University of São Paulo) for kindly lending the licenses for the ABAQUS software.

7. REFERENCES

E.J. Barbero, T.M. Damiani and J.Trovillion. 2005. Micromechanics of fabric reinforced composites with periodic microstructure, *International Journal of Solids and Structures*, 42, 2489-2504.

J.N. Reddy and O.O. Ochoa. 1993. Finite Element Analysis of Composite Laminates, *Kluwer Academic Print on Demand*, 3rd Edition.

J.N. Reddy and R.A. Arciniega, R. A. 2004. Shear deformation plate and shell theories: From Stavsky to present, Mechanics of Advanced Materials and Structures, 11(6), 535-582.

M. Sartorato and V. Tita. 2011. A finite element for composite laminated beams with a shear correction factor model, *Procedure of International Congress of Mechanical Engineering, COBEM 2011*, Natal. Brazil.

M.J. Pindera, H. Khatam, A.S. Drago and Y. Bansal. 2004. Micromechanics of spatially uniform heterogeneous media: A critical review and emerging approaches, *Composites Part-B*, 40, 349–78.

P. Potluri and V. S. Thammandra. 2007. Influence of uniaxial and biaxial tension on meso-scale geometry and strain fields in a woven composite, *Composite Structures*, 77, 405-418.

P.F. Pai. 1995. A new look at shear correction factors and warping functions of anisotropic laminates, *International Journal of Solids Structures*, 32(16), 2295-2313.

M. S. Qatu; R. W, Sullivan and W. Wand. (2010). Recent research advances on the dynamic analysis of composite shells: 2000-2009, Composite Structures, vol. 93, pp. 14-31.

P.M. Raman and J.F. Davalos. 1996. Static shear correction factor for laminated rectangular beams, *Composites Part-B*, 27B, 285-293.

Z. Xia, Y. Zhang and F. Ellyin. 2003. A unified periodical boundary conditions for representative volume elements of composites and applications, *International Journal of Solids Structures*, 40, 1907-1921.

8. RESPONSIBILITY NOTICE

The authors are the only responsible for the printed material included in this paper.